Heavy-quark self-energy in nonrelativistic lattice QCD

Colin J. Morningstar
Stanford Linear Accelerator Center, Stanford University, Stanford, California 94309
(Received 18 January 1993)

The heavy-quark self-energy in nonrelativistic lattice QCD is calculated to $O(\alpha_s)$ in perturbation theory. The heavy-quark action includes all spin-independent relativistic corrections to order v^2, where v is the typical heavy-quark velocity, and all spin-dependent corrections to order v^4. The standard Wilson action and an improved multiplaquette action are used for the gluons. Results for the mass renormalization, wave function renormalization, and energy shift are given; tadpole contributions are found to be large. A tadpole improvement scheme in which all link variables are rescaled by a mean-field factor is also studied. The effectiveness of this scheme in offsetting the large tadpole contributions to the heavy-quark renormalization parameters is demonstrated.

PACS number(s): 12.38.Gc, 11.15.Ha, 12.38.Bx

I. INTRODUCTION

A new approach to studying hadrons composed entirely of heavy quarks, called nonrelativistic lattice quantum chromodynamics (NRQCD), combines effective field theory and lattice techniques [1,2]. NRQCD is an effective field theory constructed from a set of nonrenormalizable, local interactions formulated on a space-time grid; it is essentially a low-energy expansion of the Dirac theory in terms of the expectation value v of the heavy-quark velocity in a typical heavy-quark hadron. To fully define lattice NRQCD, the coupling strengths of the interactions appearing in the action must first be specified. These are process and momentum independent and are uniquely determined (for a given regulator) by requiring that lattice NRQCD exactly reproduces the results of continuum QCD at low energies.

Since the role of these couplings is to absorb the relativistic effects arising from highly ultraviolet QCD processes, one expects that they may be computed to a good approximation using perturbation theory, provided the quark mass M is large enough. The simplest way to proceed is to evaluate various scattering amplitudes both in QCD and lattice NRQCD and adjust the couplings until these amplitudes agree to the desired order in v and the QCD coupling g. In this way, one obtains coupling coefficients which are power series in $g^2(\Lambda)$, where Λ is the cutoff of the effective theory. The cutoff Λ must be large enough so that $O(g^2(\Lambda))$ corrections to the effective couplings are small, making a perturbative analysis meaningful. However, power-law divergences generally occur, producing terms such as $g^2(\Lambda)\Lambda/M$ which render perturbation theory useless if Λ is made too large.

In this paper, the lowest-order corrections to the heavy-quark self-energy in lattice NRQCD are calculated using weak-coupling perturbation theory. Similar to an earlier study [3], the mass and wave function renormalization parameters required to match continuum QCD are obtained, as well as a necessary overall energy shift. The values of these parameters will be needed in order to extract physical information from future numerical simulations of quarkonium. In Ref. [3], only a very simple action which included no spin effects or relativistic corrections was used; here, the action formulated in Ref. [2] which includes all spin-independent relativistic interactions suppressed by v^2 relative to the leading terms and all spin-dependent corrections up to order v^4 is used. Also, a tadpole improvement scheme in which all link variables are rescaled by a mean-field factor is applied in the calculation of the heavy-quark renormalization parameters in NRQCD for the first time.

The lattice NRQCD action as determined in Ref. [2] and its improvement using link variable renormalization are briefly reviewed in Sec. II. The Feynman rules for this action are then derived in Sec. III. The self-energy calculations are presented and discussed in Sec. IV. Taking into account the mean-field corrections introduced by the tadpole improvement scheme, the coefficients of g^2 in the heavy-quark renormalization parameters are found to be small. Section V offers conclusions.

II. LATTICE NRQCD

Lattice simulations are performed in Euclidean space. The Euclidean action is obtained from the Minkowski theory by Wick rotating the contour integral of the Lagrangian over time from the real axis to the imaginary axis in a clockwise manner. Also, the path integration over the scalar potential must be similarly Wick-rotated at each point in space-time. One then defines all Euclidean-space four-vectors in terms of their corresponding Minkowski-space four-vectors using $x_4 = x^4 = ix^0_{(M)}$ and $x_j = x^j = x^j_{(M)} = -x^{(M)}_j$, for $j = 1,2,3$, except for the derivative operator and the gauge fields which are defined using $\partial_4 = \partial^4 = -i\partial^{(M)}_0$, $\partial_j = \partial^j = \partial^{(M)}_j = -\partial^j_{(M)}$ and $A_4 = A^4 = -iA^0_{(M)}$, $A_j = A^j = A^{(M)}_j = -A^j_{(M)}$. With these definitions, the quantities x_μ and $A_\mu(x)$ are then real and the Minkowski-space metric tensor $g_{\mu\nu} = \mathrm{diag}(1,-1,-1,-1)$ transforms into the identity matrix in Euclidean space. The path integral weight $\exp(iS)$ becomes $\exp(-S_E)$, where S_E is the Euclidean action.

In lattice NRQCD, the heavy-quark field $\psi(x)$ is defined on the sites of a four-dimensional hypercubic lattice with spacing a and is a Pauli spinor corresponding to the two upper components of the usual Dirac field. The gauge-field degrees of freedom reside on the links between the sites. With each link originating at a site x and terminating at a site $x + a\hat{e}_\mu$ is associated a link variable $U_\mu(x)$, which is a lattice version of the parallel transport matrix between sites and is an element of the Lie group associated with the gauge invariance of the theory. Covariant differences are defined by

$$a\Delta_\mu^{(+)}\psi(x) = U_\mu(x)\psi(x + a\hat{e}_\mu) - \psi(x), \tag{1}$$

$$a\Delta_\mu^{(-)}\psi(x) = \psi(x) - U_\mu^\dagger(x - a\hat{e}_\mu)\psi(x - a\hat{e}_\mu), \tag{2}$$

$$\Delta^{(\pm)} = \frac{1}{2}(\Delta^{(+)} + \Delta^{(-)}), \tag{3}$$

and the Laplacian is given by

$$\mathbf{\Delta}^{(2)} = \sum_{k=1}^{3} \Delta_k^{(+)}\Delta_k^{(-)} = \sum_{k=1}^{3} \Delta_k^{(-)}\Delta_k^{(+)}. \tag{4}$$

An improved difference operator which reproduces the behavior of the continuum covariant derivative through order a^4 is given by

$$\tilde{\Delta}_k^{(\pm)} = \Delta_k^{(\pm)} - \frac{a^2}{6}\Delta_k^{(+)}\Delta_k^{(\pm)}\Delta_k^{(-)}, \tag{5}$$

and an improved lattice Laplacian is

$$\tilde{\mathbf{\Delta}}^{(2)} = \mathbf{\Delta}^{(2)} - \frac{a^2}{12}\sum_{k=1}^{3}\left(\Delta_k^{(+)}\Delta_k^{(-)}\right)^2. \tag{6}$$

The Hermitian and traceless field strength tensor is best represented [4] by cloverleaf operators defined at the sites of the lattice:

$$F_{\mu\nu}(x) = \mathcal{F}_{\mu\nu}(x) - \frac{1}{3}\mathrm{Tr}\mathcal{F}_{\mu\nu}(x), \tag{7}$$

$$\mathcal{F}_{\mu\nu}(x) = \frac{-i}{2a^2 g}\left(\Omega_{\mu\nu}(x) - \Omega_{\mu\nu}^\dagger(x)\right), \tag{8}$$

$$\Omega_{\mu\nu}(x) = \frac{1}{4}\sum_{\{(\alpha,\beta)\}_{\mu\nu}} U_\alpha(x)U_\beta(x + a\hat{e}_\alpha) \times U_{-\alpha}(x + a\hat{e}_\alpha + a\hat{e}_\beta)U_{-\beta}(x + a\hat{e}_\beta), \tag{9}$$

with $\{(\alpha,\beta)\}_{\mu\nu} = \{(\mu,\nu),(\nu,-\mu),(-\mu,-\nu),(-\nu,\mu)\}$ for $\mu \neq \nu$. This representation is chosen since it transforms as the $(1,0) \oplus (0,1)$ six-dimensional reducible representation of the hypercubic group, similar to the continuum case. The chromoelectric and chromomagnetic fields in Euclidean space are defined by $E^k(x) = F_{k4}(x) = -F_{4k}(x)$ and $B^k(x) = -\frac{1}{2}\epsilon_{klm}F_{lm}(x)$, where $\epsilon_{123} = 1$. An improved cloverleaf field strength tensor may be defined by

$$\tilde{F}_{\mu\nu}(x) = \frac{5}{3}F_{\mu\nu}(x) - \frac{1}{6}[U_\mu(x)F_{\mu\nu}(x + a\hat{e}_\mu)U_\mu^\dagger(x) + U_\mu^\dagger(x - a\hat{e}_\mu)F_{\mu\nu}(x - a\hat{e}_\mu)U_\mu(x - a\hat{e}_\mu) - (\mu \leftrightarrow \nu)]. \tag{10}$$

The portion of the lattice NRQCD action containing the heavy-quark–gluon interactions may be written [2]

$$S_Q^{(n)} = a^3\sum_x \psi^\dagger(x)\psi(x) - a^3\sum_x \psi^\dagger(x + a\hat{e}_4)\left(1 - \frac{a\tilde{H}_0}{2n}\right)^n\left(1 - \frac{a\delta H}{2}\right) \times U_4^\dagger(x)\left(1 - \frac{a\delta H}{2}\right)\left(1 - \frac{a\tilde{H}_0}{2n}\right)^n\psi(x), \tag{11}$$

where n is a positive integer, the improved kinetic energy is given by

$$\tilde{H}_0 = -\frac{\tilde{\mathbf{\Delta}}^{(2)}}{2M} - \frac{a}{4n}\frac{(\mathbf{\Delta}^{(2)})^2}{4M^2}, \tag{12}$$

and the quark-gluon interactions are

$$\delta H = \sum_{j=1}^{7} c_j\, V_j, \tag{13}$$

where

$$V_1 = -\frac{(\mathbf{\Delta}^{(2)})^2}{8M^3}, \tag{14}$$

$$V_2 = \frac{ig}{8M^2}\left(\mathbf{\Delta}^{(\pm)}\cdot\mathbf{E} - \mathbf{E}\cdot\mathbf{\Delta}^{(\pm)}\right), \tag{15}$$

$$V_3 = -\frac{g}{8M^2}\boldsymbol{\sigma}\cdot(\tilde{\mathbf{\Delta}}^{(\pm)}\times\tilde{\mathbf{E}} - \tilde{\mathbf{E}}\times\tilde{\mathbf{\Delta}}^{(\pm)}), \tag{16}$$

$$V_4 = -\frac{g}{2M}\boldsymbol{\sigma}\cdot\tilde{\mathbf{B}}, \tag{17}$$

$$V_5 = -\frac{g}{8M^3}\{\mathbf{\Delta}^{(2)}, \boldsymbol{\sigma}\cdot\mathbf{B}\}, \tag{18}$$

$$V_6 = -\frac{3g}{64M^4}\{\mathbf{\Delta}^{(2)}, \boldsymbol{\sigma}\cdot(\mathbf{\Delta}^{(\pm)}\times\mathbf{E} - \mathbf{E}\times\mathbf{\Delta}^{(\pm)})\}, \tag{19}$$

$$V_7 = -\frac{ig^2}{8M^3}\boldsymbol{\sigma}\cdot\mathbf{E}\times\mathbf{E}. \tag{20}$$

The parameter n was introduced in Ref. [1] to remove instabilities in the evolution of the quark Green's function which occur when the temporal spacing is not small enough to accurately treat the high-momentum modes, and the coefficients c_j are functions of aM and the coupling g in general. At the tree level, their values are all unity. Note that the three-vector $\mathbf{\Delta}^{(\pm)}$ refers to the spatial components of the covariant four-vector $\Delta_\mu^{(\pm)}$, while $\mathbf{E}$ and $\mathbf{B}$ refer to the components E^k and B^k, respectively.

The standard Euclidean gluon action is given by

$$\hat{S}_G = a^4\sum_x \mathcal{L}_G(x), \tag{21}$$

where

$$\mathcal{L}_G(x) = \frac{1}{2a^4g^2}\sum_{\mu\neq\nu}\mathrm{Tr}\left[2 - \Omega_{\mu\nu}(x) - \Omega_{\mu\nu}^\dagger(x)\right] \tag{22}$$

is the usual single-plaquette lattice gauge-field Lagrangian density. An improved gluonic action may be written

$$S_G = a^4 \sum_x \left(\frac{4}{3}\mathcal{L}_G(x) - \frac{1}{3}\mathcal{L}_G^{(2\times 2)}(x) \right), \tag{23}$$

where $\mathcal{L}_G^{(2\times 2)}$ is comprised of 2×2 plaquette operators and is given by

$$\mathcal{L}_G^{(2\times 2)}(x) = \frac{1}{32a^4 g^2} \sum_{\mu\neq\nu} \mathrm{Tr}\left[2 - \Omega_{\mu\nu}^{(2)}(x) - \Omega_{\mu\nu}^{\dagger(2)}(x)\right], \tag{24}$$

with

$$\begin{aligned}\Omega_{\mu\nu}^{(2)}(x) = \frac{1}{4} \sum_{\{(\alpha,\beta)\}_{\mu\nu}} & U_\alpha(x) U_\alpha(x+a\hat{e}_\alpha) \\ & \times U_\beta(x+2a\hat{e}_\alpha) U_\beta(x+2a\hat{e}_\alpha+a\hat{e}_\beta) \\ & \times U_{-\alpha}(x+2a\hat{e}_\alpha+2a\hat{e}_\beta) U_{-\alpha}(x+a\hat{e}_\alpha+2a\hat{e}_\beta) \\ & \times U_{-\beta}(x+2a\hat{e}_\beta) U_{-\beta}(x+a\hat{e}_\beta),\end{aligned} \tag{25}$$

and $\{(\alpha,\beta)\}_{\mu\nu} = \{(\mu,\nu),(\nu,-\mu),(-\mu,-\nu),(-\nu,\mu)\}$ for $\mu \neq \nu$. Presently, light quarks are neglected.

The lattice NRQCD action is formulated in terms of the link variables $U_\mu(x)$ in order to preserve local gauge invariance, and as the lattice spacing a becomes small, it must tend to the action of the continuum theory. This can be shown at tree level in perturbation theory using the following relationship between the link variables and the gluon field $G_\mu(x)$ of the continuum theory:

$$U_\mu(x) \equiv \exp\left[iagA_\mu\left(x + \frac{a}{2}\hat{e}_\mu\right)\right] \sim 1 + iagG_\mu(x), \tag{26}$$

where the lattice gluon field $A_\mu(x) = G_\mu(x) + O(a^2)$. Beyond the tree level, however, one observes that large renormalizations are necessary to match the small a limit of the lattice action to the continuum form. These large renormalizations stem mainly from the higher-order powers of agA_μ which occur in the expansion of U_μ. Such terms generate ultraviolet divergences proportional to powers of a^{-1} and so are suppressed only by powers of g^2 and not a.

A simple gauge-invariant procedure for improving the lattice NRQCD action by reducing the magnitudes of the renormalizations needed to reproduce the continuum theory has been suggested: replace all link variables U_μ that appear in the lattice action by U_μ/u_0, where u_0 is a parameter representing the mean value of the link [2]. A gauge-invariant definition of this mean-field parameter may be written in terms of the mean plaquette:

$$u_0 = \langle \tfrac{1}{3}\mathrm{Tr}U_{\mathrm{plaq}}\rangle^{1/4}. \tag{27}$$

The parameter u_0 may be calculated using perturbation theory or may be measured in a simulation in order to include nonperturbative effects.

III. THE FEYNMAN RULES

To facilitate the perturbative evaluation of scattering amplitudes, a lattice gluon field $A_\mu(x) = \sum_{b=1}^{8} A_\mu^b(x) T^b$ is defined in terms of the link variables using

$$U_\mu(x) \equiv \exp\left[iagA_\mu\left(x + \frac{a}{2}\hat{e}_\mu\right)\right], \tag{28}$$

where $(\hat{e}_\mu)_\alpha = \delta_{\mu\alpha}$. The gauge-invariant path integral measure must then be expressed in terms of the lattice gluon field [5]:

$$[\mathcal{D}U] = \exp\left(-S_{\mathrm{ms}}\right) \left(\prod_{xb\mu} dA_\mu^b(x) \right), \tag{29}$$

where

$$S_{\mathrm{ms}} = -\frac{1}{2} \sum_{x\mu} \mathrm{Tr}\ln\left[\frac{2[1-\cos ag\mathcal{A}_\mu(x+\frac{a}{2}\hat{e}_\mu)]}{[ag\mathcal{A}_\mu(x+\frac{a}{2}\hat{e}_\mu)]^2} \right] \tag{30}$$

and $\mathcal{A}_\mu^{bc} = if^{bcd}A_\mu^d$. To order g^2,

$$S_{\mathrm{ms}} \approx \frac{a^2 g^2}{8} \sum_{xb\mu} \left[A_\mu^b\left(x + \frac{a}{2}\hat{e}_\mu\right)\right]^2. \tag{31}$$

In a lattice gauge theory, the space of gauge transformations is finite so that gauge fixing is not necessary. However, weak-coupling perturbation theory can only be applied if one fixes the gauge and extends the integration range of $A_\mu^b(x)$ using the familiar Faddeev-Popov technique [6]. Hence, a gauge-fixing term S_{GF} must be added to the NRQCD action. The Faddeev-Popov ghost action can then be determined from S_{GF} [7].

The Feynman rules are determined by expanding the total action in terms of the coupling g and Fourier transforming into momentum space. The coupling coefficients are written $c_j = 1 + g^2 c_j^{(2)} + O(g^4)$. Rewriting the heavy-quark–gluon action as

$$S_Q^{(n)} = a^8 \sum_{xy} \psi^\dagger(y) G(y;x) \psi(x), \tag{32}$$

then

$$S_Q^{(n)} = \int \frac{d^4k}{(2\pi)^4} \frac{d^4k'}{(2\pi)^4}\, \tilde{\psi}^\dagger(k') \tilde{G}(k';k) \tilde{\psi}(k), \tag{33}$$

where the Fourier transforms are defined on an infinite lattice by

$$\psi(x) = \int_{|k_\mu|\leq \pi/a} \frac{d^4k}{(2\pi)^4} e^{ik\cdot x} \tilde{\psi}(k), \tag{34}$$

$$\tilde{G}(k';k) = a^8 \sum_{xy} e^{-ik'\cdot y + ik\cdot x} G(y;x). \tag{35}$$

The perturbative expansion of $\tilde{G}(k';k)$ in terms of the gluon fields takes the general form:

$$\tilde{G}(k';k) = (2\pi)^4\delta^{(4)}(k'-k)\; a^{-1}\xi^{(0)}_{\tilde{G}}(k',k) + \sum_{\nu_1 b_1}\int d(k',k;q_1)\;\tilde{A}^{b_1}_{\nu_1}(q_1) \times\xi^{(1)}_{\tilde{G}}(k',k;q_1,\nu_1,b_1) + \sum_{\nu_1\nu_2 b_1 b_2}\int d(k',k;q_1,q_2)\;\tilde{A}^{b_1}_{\nu_1}(q_1)\tilde{A}^{b_2}_{\nu_2}(q_2) \times a\xi^{(2)}_{\tilde{G}}(k',k;q_1,\nu_1,b_1;q_2,\nu_2,b_2) + \cdots, \quad (36)$$

where

$$d(k',k;q_1,\ldots,q_r) = \left[\prod_{i=1}^{r}\frac{d^4q_i}{(2\pi)^4}\right](2\pi)^4\delta^{(4)}\left(k'-k+\sum_{i=1}^{r}q_i\right) \quad (37)$$

and $\tilde{A}_\mu(q)$ is the Fourier transform of $A_\mu(x)$ defined by

$$A_\mu(x) = \int\frac{d^4q}{(2\pi)^4}e^{-iq\cdot x}\tilde{A}_\mu(q). \quad (38)$$

Thus, the Feynman rules follow easily from the (dimensionless) $\xi^{(i)}_{\tilde{G}}$ functions.

One of the simplest ways to compute the functions $\xi^{(i)}_{\tilde{G}}$ is to first calculate the Fourier transforms of the basic operators which comprise $\tilde{G}(k';k)$ and then combine these Fourier transforms appropriately. The perturbative expansion of the transform of each such operator will take the same general form as that for $\tilde{G}(k';k)$ given above. Of course, this general form also applies to transform products. Let

$$C_{\{\alpha\beta\}}(k';k) = \int\frac{d^4p}{(2\pi)^4}\;A_{\{\alpha\}}(k';p)\;B_{\{\beta\}}(p;k), \quad (39)$$

then the product rule for the ξ functions may be expressed as

$$\xi^{(r)}_{C_{\{\alpha\beta\}}}\left(k',k;\{q_l,\nu_l,b_l\}_{l=1}^{r}\right) = \sum_{s=0}^{r}\xi^{(s)}_{A_{\{\alpha\}}}\left(k',k'+\sum_{l=1}^{s}q_l;\{q_i,\nu_i,b_i\}_{i=1}^{s}\right) \times\xi^{(r-s)}_{B_{\{\beta\}}}\left(k-\sum_{m=s+1}^{r}q_m,k;\{q_j,\nu_j,b_j\}_{j=s+1}^{r}\right). \quad (40)$$

Using this rule and the additivity of the ξ functions, one can quickly build up the $\xi^{(i)}_{\tilde{G}}$ functions. The Fourier transforms of all the necessary basic operators are presented in the Appendix.

The lowest-order heavy-quark propagator, shown in Fig. 1(a), is given by

$$\mathcal{Q}^{ij}_{\alpha\beta}(k) = a\delta^{ij}\delta_{\alpha\beta}Q(k), \quad (41)$$

where i,j are color indices and α,β are spin indices, and

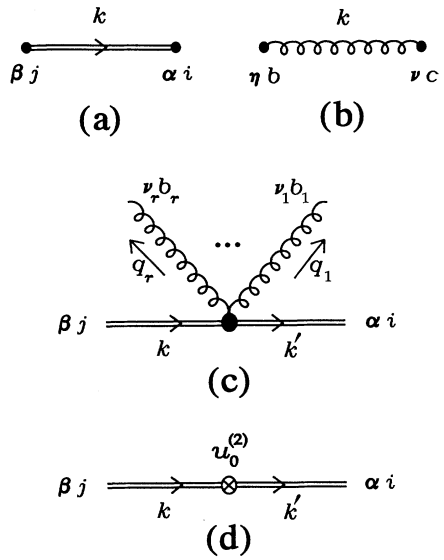

FIG. 1. Various Feynman diagram elements. A curly line represents a gluon; a double solid line indicates a heavy quark. (a) Heavy-quark propagator; (b) gluon propagator; (c) lowest-order vertices involving a heavy-quark line and r gluons; (d) the $O(g^2)$ counterterm from link variable renormalization.

$$Q(k) = \left[1-e^{-ik_4a}\left(1+\frac{\kappa_2(\mathbf{k})^2}{M^3a^3}\right)^2 \times\left(1-\frac{\kappa_2(\mathbf{k})}{nMa}-\frac{\kappa_4(\mathbf{k})}{3nMa}+\frac{\kappa_2(\mathbf{k})^2}{2n^2M^2a^2}\right)^{2n}\right]^{-1} \quad (42)$$

with $\kappa_n(\mathbf{k}) = \sum_{j=1}^{3}\sin^n(k_ja/2)$.

In the Feynman gauge, the lowest-order gluon propagator, shown in Fig. 1(b), is given by

$$\mathcal{D}^{bc}_{\eta\nu}(k;\lambda) = a^2\delta^{bc}\delta_{\eta\nu}D_\nu(k;\lambda), \quad (43)$$

where

$$D_\nu(k;\lambda) = \left[\frac{16}{3}\left(\sum_{\alpha=1}^{4}\sin^2\left(\frac{k_\alpha a}{2}\right)\right) -\frac{1}{3}\cos^2\left(\frac{k_\nu a}{2}\right)\left(\sum_{\alpha=1}^{4}\sin^2(k_\alpha a)\right)+a^2\lambda^2\right]^{-1}. \quad (44)$$

A small gluon mass λ has been introduced to provide an infrared cutoff. If the simple gluon action in Eq. (21) is used, the lowest-order gluon propagator is then

$$\hat{\mathcal{D}}^{bc}_{\eta\nu}(k;\lambda) = a^2\delta^{bc}\delta_{\eta\nu}\hat{D}(k;\lambda), \quad (45)$$

where

$$\hat{D}(k;\lambda) = \left[4\left(\sum_{\alpha=1}^{4}\sin^2\left(\frac{k_\alpha a}{2}\right)\right)+a^2\lambda^2\right]^{-1}. \quad (46)$$

The lowest-order vertex factors corresponding to interactions involving a heavy-quark line and one to three gluons, shown in Fig. 1(c), may be written

$$\mathcal{V}_1(k',\alpha,i;k,\beta,j;q_1,\nu_1,b_1) = -g(2\pi)^4\delta^{(4)}\Big(k'-k+q_1\Big)\sum_{\mu=1}^{4}\sigma^{\mu}_{\alpha\beta}\,T^{b_1}_{ij}\,\zeta^{(1)}_{\tilde{G}_0\mu}\big(k',k;q_1,\nu_1\big), \tag{47}$$

$$\mathcal{V}_2(k',\alpha,i;k,\beta,j;q_1,\nu_1,b_1;q_2,\nu_2,b_2) = -ag^2\,(2\pi)^4\delta^{(4)}\Big(k'-k+q_1+q_2\Big) \times\sum_{\mu=1}^{4}\sigma^{\mu}_{\alpha\beta}\sum_{\tau\in\mathcal{P}_2}\Big(T^{b_{\tau_1}}T^{b_{\tau_2}}\Big)_{ij}\zeta^{(2)}_{\tilde{G}_0\mu}\big(k',k;q_{\tau_1},\nu_{\tau_1};q_{\tau_2},\nu_{\tau_2}\big), \tag{48}$$

$$\mathcal{V}_3(k',\alpha,i;k,\beta,j;q_1,\nu_1,b_1;q_2,\nu_2,b_2;q_3,\nu_3,b_3) = -a^2g^3\,(2\pi)^4\delta^{(4)}\Big(k'-k+q_1+q_2+q_3\Big) \times\sum_{\mu=1}^{4}\sigma^{\mu}_{\alpha\beta}\sum_{\tau\in\mathcal{P}_3}\Bigg[\Big(T^{b_{\tau_1}}T^{b_{\tau_2}}T^{b_{\tau_3}}\Big)_{ij}\zeta^{(3a)}_{\tilde{G}_0\mu}\big(k',k;q_{\tau_1},\nu_{\tau_1};q_{\tau_2},\nu_{\tau_2};q_{\tau_3},\nu_{\tau_3}\big) +\delta_{ij}\,\mathrm{Tr}\Big(T^{b_{\tau_1}}T^{b_{\tau_2}}T^{b_{\tau_3}}\Big)\zeta^{(3b)}_{\tilde{G}_0\mu}\big(k',k;q_{\tau_1},\nu_{\tau_1};q_{\tau_2},\nu_{\tau_2};q_{\tau_3},\nu_{\tau_3}\big)\Bigg], \tag{49}$$

where $\mathcal{P}_r$ is the group of permutations of r elements, σ^k are the standard Pauli spin matrices for $k=1,2,3$ and σ^4 is a 2×2 identity matrix in spin space. The $\zeta_{\tilde{G}_0}$ functions are obtained from the $\xi_{\tilde{G}}$ functions by neglecting the $O(g^2)$ corrections to the c_j coupling coefficients. These corrections show up in higher-order counterterms. Link variable renormalization in perturbation theory leads to the addition of the following order g^2 counterterm, shown in Fig. 1(d):

$$\begin{aligned}\mathcal{V}_{u_0}(k',\alpha,i;k,\beta,j) = -u_0^{(2)}\,\frac{g^2}{a}(2\pi)^4\delta^{(4)}\Big(k'-k\Big)\delta_{\alpha\beta}\delta_{ij}e^{-ik_4a} &\times\left(1-\frac{\kappa_2(\mathbf{k})}{nMa}-\frac{\kappa_4(\mathbf{k})}{3nMa}+\frac{\kappa_2(\mathbf{k})^2}{2n^2M^2a^2}\right)^{2n-1}\left(1+\frac{\kappa_2(\mathbf{k})^2}{M^3a^3}\right)\\ &\times\Bigg\{\left(1-\frac{6\kappa_2(\mathbf{k})}{M^3a^3}+\frac{5\kappa_2(\mathbf{k})^2}{M^3a^3}\right)\left(1-\frac{\kappa_2(\mathbf{k})}{nMa}-\frac{\kappa_4(\mathbf{k})}{3nMa}+\frac{\kappa_2(\mathbf{k})^2}{2n^2M^2a^2}\right)\\ &\quad+\left(1+\frac{\kappa_2(\mathbf{k})^2}{M^3a^3}\right)\left(\frac{7}{2Ma}-\frac{4\kappa_2(\mathbf{k})}{3Ma}-\frac{4\kappa_4(\mathbf{k})}{3Ma}-\frac{3\kappa_2(\mathbf{k})}{nM^2a^2}+\frac{2\kappa_2(\mathbf{k})^2}{nM^2a^2}\right)\Bigg\},\end{aligned} \tag{50}$$

writing $u_0 = 1 + u_0^{(2)}g^2 + O(g^4)$.

The goal here is to determine the numerical values of the coupling coefficients c_j and d_j and various renormalization factors for given values of the input parameters needed in lattice simulations: namely, the bare lattice coupling g and the bare heavy-quark mass aM. Since these couplings and renormalization factors essentially absorb the relativistic effects arising from highly ultraviolet processes, one expects that they may be calculated to a good approximation using weak-coupling perturbation theory. Using the above Feynman rules, the development of perturbative expansions for these quantities in terms of g is straightforward. However, there is no compelling reason to use the bare lattice coupling for the expansion parameter. In fact, recent work [8] suggests that g is a very poor choice of expansion parameter and that much better perturbation series result if one reexpresses the series in terms of a renormalized coupling g_r defined in terms of some physical quantity and which runs with the relevant length scale. This is standard practice in continuum perturbation theory. Of course, if calculations could be carried out to all orders, then the choice of expansion parameter would be immaterial.

To define a renormalized expansion parameter, a definition of the running coupling $g_r(\mu)$ and a procedure for determining the relevant mass scale μ must be given. A renormalization scheme [8] which defines the coupling such that the heavy-quark potential has no g_r^4 or higher-order corrections is particularly attractive. This scheme is physically motivated and produces $O(g_r^2)$ perturbative results in good agreement with simulation results for several different quantities. By absorbing the higher-order contributions to the heavy-quark potential into g_r^2, it is hoped that higher-order contributions in other quantities will be small. The renormalized coupling $g_r(\mu)$ is then given by the usual two-loop formula with $\Lambda = 46.08\Lambda_{\mathrm{lat}}$. The scale μ is determined by averaging $\ln q^2$ over the one-loop process of interest, where q is the loop momentum. Since the heavy-quark parameters calculated here are ultraviolet divergent quantities, one expects $\mu \approx \pi/a$. Here, $\bar{g}_r$ shall be used to denote the value $g_r(\mu)$ of the renormalized coupling at the appropriate scale. For example, at $\beta = 5.7$, $g_r^2(\pi/a) \approx 1.9$ and at $\beta = 6.0$, $g_r^2(\pi/a) \approx 1.7$. Alternatively, $\bar{g}_r$ could simply be added to the list of parameters which must be fixed in any simulation by reference to experiment.

IV. THE HEAVY-QUARK SELF-ENERGY

The heavy-quark self-energy $\Sigma(p)$ may be defined by writing the inverse quark propagator $\mathcal{G}^{-1}(p)$ in the form

$$a\mathcal{G}^{-1}(p)^{ij}_{\alpha\beta} = Q^{-1}(p)\delta^{ij}\delta_{\alpha\beta} - a\Sigma^{ij}_{\alpha\beta}(p), \tag{51}$$

where i,j are color indices and α,β are spin indices. At order g^2 and v^4 and neglecting link variable renormalization for the moment, this self-energy is given by

$$\Sigma^{ij}_{\alpha\beta}(p) = \lim_{\lambda\to 0} g^2\delta^{ij}\delta_{\alpha\beta}\big(\Sigma^{(A)}(p;\lambda) + \Sigma^{(B)}(p;\lambda)\big), \tag{52}$$

where

$$a\Sigma^{(A)}(p;\lambda) = \frac{4}{3}a^4 \sum_{\mu,\nu=1}^{4} \int \frac{d^4k}{(2\pi)^4} Q(p-k) \times D_\nu(k;\lambda)\ \varepsilon_\mu\big[\zeta^{(1)}_{\tilde{G}_0\mu}(p-k,p;k,\nu)\big]^2, \tag{53}$$

corresponding to the diagram in Fig. 2(a), and

$$a\Sigma^{(B)}(p;\lambda) = -\frac{4}{3}a^4 \sum_{\nu=1}^{4} \int \frac{d^4k}{(2\pi)^4} D_\nu(k;\lambda) \times \zeta^{(2)}_{\tilde{G}_0 4}(p,p;k,\nu;-k,\nu), \tag{54}$$

corresponding to the tadpole diagram in Fig. 2(b). Note that $\varepsilon_\mu = (-1,-1,-1,1)$. The following properties of the ζ functions are used to obtain the above results:

$$\zeta^{(1)}_{\tilde{G}_0\mu}(k',k;k-k',\nu) = \varepsilon_\mu\ \zeta^{(1)}_{\tilde{G}_0\mu}(k,k';k'-k,\nu), \tag{55}$$

$$\zeta^{(2)}_{\tilde{G}_0 j}(p,p;k,\nu;-k,\nu) = 0 \quad (j=1,2,3). \tag{56}$$

The self-energy is invariant under interchange of any two spatial components $p_i \leftrightarrow p_j$ and spatial reflections $p_j \to -p_j$, for $i,j = 1,2,3$, and transforms into its complex conjugate under $p_4 \to -p_4^*$.

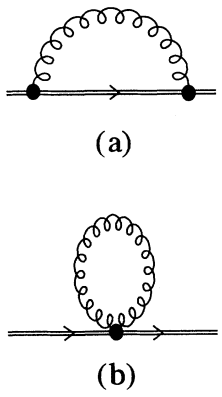

FIG. 2. Two Feynman diagrams which contribute to the heavy-quark self-energy. A curly line denotes a gluon; a double solid line denotes a heavy quark.

In order to investigate $\Sigma^{(A)}(p;\lambda)$ and $\Sigma^{(B)}(p;\lambda)$ in the neighborhood of $p = 0$, the integrals in Eqs. (53) and (54) must first be evaluated. The usual initial step in the determination of such integrals is to use the change of variables $z = \exp(\pm ik_4 a)$ to transform the integral over k_4 into a contour integral along the $|z| = 1$ unit circle. Unfortunately, the complicated pole structure of the vertex factors near $z = 0$ makes difficult the evaluation of this contour integral by the residue theory. Because of this fact, the simplest procedure, approximating the four-dimensional integral by an appropriate summation as described below, is preferred.

Because the integrand in Eq. (54) is a periodic analytic function of the real variables k_μ with period 2π when $\lambda > 0$, $\Sigma^{(B)}(p;\lambda)$ is numerically well approximated by the discrete sum

$$a\Sigma^{(B)}(p;\lambda) \approx -\frac{4}{3}\frac{1}{N^4}\sum_{k}\sum_{\nu=1}^{4} D_\nu(k;\lambda) \times \zeta^{(2)}_{\tilde{G}_0 4}(p,p;k,\nu;-k,\nu). \tag{57}$$

In this sum, $ak_\mu = 2\pi n_\mu/N$ where the n_μ take all integer values satisfying $-N/2 < n_\mu \le N/2$ for integral N. The error resulting from this approximation diminishes exponentially fast as $N \to \infty$. However, the rate of decay of this error is directly proportional to the mass gap $a\lambda$, creating difficulties when $a\lambda$ is small. Fortunately, the decay rate of this error can be dramatically increased by making the following change of variables [9]: $k_\mu \to k_\mu - \alpha\sin(k_\mu)$ with $0 \le \alpha < 1$. This transformation maintains periodicity and effectively increases the mass gap so that the approximation

$$a\Sigma^{(B)}(p;\lambda) \approx -\frac{4}{3}\frac{1}{N^4}\sum_{k}\sum_{\nu=1}^{4} \varrho(k) D_\nu(s(k);\lambda) \times \zeta^{(2)}_{\tilde{G}_0 4}(p,p;s(k),\nu;-s(k),\nu), \tag{58}$$

where $s_\mu(k) = k_\mu - \alpha\sin(k_\mu)$ and $\varrho(k) = \prod_{\mu=1}^{4}[1 - \alpha\cos(k_\mu)]$, converges much more quickly as N is increased. The parameter α should be chosen so as to maximize the effective mass gap: $\alpha = \mathrm{sech}(u)$, where u satisfies $a\lambda \approx u - \tanh(u)$.

The above procedure is sufficient for evaluating $\Sigma^{(B)}(p;\lambda)$ as long as the gluon mass $a\lambda$ is not set too small. However, the singularity in the quark propagator is problematical when evaluating $\Sigma^{(A)}(p;\lambda)$ near $p = 0$. To circumvent this, the contour for the ak_4 integral, which runs along the real axis from $-\pi$ to π except near the singularity, can be continuously deformed into a contour consisting of three line segments passing through the points $-\pi \to -\pi + ia\lambda/2 \to \pi + ia\lambda/2 \to \pi$. This contour is chosen for the following two reasons: for $p \sim 0$, the distance of closest approach to any singularity is a maximum; and the contributions from the segments of the contour running parallel to the imaginary axis cancel due to the periodicity of the integrand. $\Sigma^{(A)}(p \sim 0;\lambda)$ can then be accurately obtained using the approximation

$$a\Sigma^{(A)}(p\sim 0;\lambda) \approx \frac{4}{3}\frac{1}{N^4}\sum_k \sum_{\mu,\nu=1}^{4} \varrho(k) Q\big(p-r(k)\big) D_\nu\big(r(k);\lambda\big)\varepsilon_\mu \Big[\zeta^{(1)}_{\tilde{G}_0\mu}\big(p-r(k),p;r(k),\nu\big)\Big]^2, \tag{59}$$

where $r_\mu(k) = k_\mu - \alpha\sin(k_\mu) + ia\lambda\delta_{4,\mu}/2$ and $ak_\mu = 2\pi n_\mu/N$ with the n_μ taking all integer values satisfying $-N/2 < n_\mu \le N/2$. Also, $\alpha = \mathrm{sech}(y)$ and $a\lambda/2 \approx y - \tanh(y)$. In practice, the approximations in Eqs. (58) and (59) are applied using increasing values of N until sufficient convergence is observed; typically, $N = 20$ is adequate. Note that for values of p satisfying $p_x = p_y = p_z$, the number of terms which must be independently evaluated in these sums may be dramatically reduced by exploiting the invariance of the summands under interchange of any two spatial components of k.

The evaluation of $\Sigma^{(A)}(p\sim 0;\lambda)$ and $\Sigma^{(B)}(p\sim 0;\lambda)$ using Eqs. (59) and (58) is feasible only if the gluon mass λ is not set too small. However, the limits of these functions as $\lambda \to 0$ are actually required, necessitating the use of an extrapolation procedure. The expected behavior of these quantities as λ tends to zero may be expressed as an asymptotic expansion of the form

$$\Sigma(p;\lambda) \underset{\lambda\to 0+}{\sim} \sum_{m=0}^{\infty}\left(b_m^{(0)} + b_m^{(1)}\ln a^2\lambda^2\right)(a\lambda)^m, \tag{60}$$

where the coefficient $b_0^{(1)}$ is known from the continuum theory since the infrared divergence is insensitive to the ultraviolet regulator. If one neglects the $b_m^{(1)}$ terms for $m > 0$, then polynomial extrapolation using Neville's algorithm may be applied to $f_0(p;\lambda) = \Sigma(p;\lambda) - b_0^{(1)}\ln a^2\lambda^2$. The extrapolation can be improved by applying Neville's algorithm to the function $f_1(p;\lambda) = f_0(p;\lambda) - a\lambda\partial_{(a\lambda)}\Sigma(p;\lambda) + 2b_0^{(1)}$ which has no $a\lambda\ln a^2\lambda^2$ term. Polynomial extrapolation of $f_2(p;\lambda) = f_1(p;\lambda) + (a^2\lambda^2/2)\partial^2_{(a\lambda)}\Sigma(p;\lambda) + b_0^{(1)}$, which does not suffer from $a^2\lambda^2\ln a^2\lambda^2$ and $a\lambda\ln a^2\lambda^2$ effects, is another method. Since the gluon mass appears only in the gluon propagator, the derivatives of $\Sigma(p;\lambda)$ with respect to $a\lambda$ can be exactly and efficiently taken. In practice, polynomial extrapolation of all three functions $f_0(p;\lambda)$, $f_1(p;\lambda)$, and $f_2(p;\lambda)$ is done using between six and twelve values of the gluon mass lying in the range $0.15 \le a\lambda \le 0.8$, and agreement among the results is verified. In calculating $\Sigma^{(B)}(p;\lambda\to 0)$, one finds that only even powers of $a\lambda$ occur in its asymptotic expansion. In this case, the accuracy of the extrapolation can be increased by explicitly excluding the odd powers in the extrapolating polynomial. Neville's algorithm is then applied to the functions $f_0(p;\lambda)$, $\tilde{f}_1(p;\lambda) = f_0(p;\lambda) - a^2\lambda^2\partial_{(a^2\lambda^2)}\Sigma(p;\lambda) + b_0^{(1)}$ and $\tilde{f}_2(p;\lambda) = \tilde{f}_1(p;\lambda) + (a^4\lambda^4/2)\partial^2_{(a^2\lambda^2)}\Sigma(p;\lambda) + b_0^{(1)}/2$. Uncertainties in the extrapolated values are estimated by examining the spread of values in the Neville table and by comparing the results obtained using different sets of gluon mass values and using the different functions described above.

The small v expansion of the zeroth-order heavy-quark inverse propagator, keeping only those terms which are suppressed by no more than v^2 relative to the leading terms, is given by

$$Q^{-1}(p) \approx ip_4 a + \frac{\mathbf{p}^2a^2}{2Ma} + \frac{p_4^2a^2}{2} - \frac{ip_4\mathbf{p}^2a^3}{2Ma} - \frac{(\mathbf{p}^2)^2a^4}{8M^3a^3} - \frac{(\mathbf{p}^2)^2a^4}{8M^2a^2} + \cdots, \tag{61}$$

recalling that p_4 is of order v^2. The on-mass-shell quark then satisfies the dispersion relation

$$\omega_0(\mathbf{p}) \approx i\Big(\frac{\mathbf{p}^2}{2M} - \frac{(\mathbf{p}^2)^2}{8M^3} + \cdots\Big), \tag{62}$$

where $\omega_0(\mathbf{p})$ denotes the value of p_4 at the singularity of the zeroth-order propagator. This dispersion relation agrees exactly with the continuum form from full QCD to this order in v.

In the modified minimal subtraction ($\overline{\mathrm{MS}}$) renormalization scheme, the inverse propagator to order g^2 for full QCD in continuum Minkowski space has the form

$$(1 - C_{\mathrm{cont}}g^2)\left[\not{p} - M(1+\delta_{\mathrm{cont}}g^2)\right] \tag{63}$$

where

$$C_{\mathrm{cont}} = \frac{1}{12\pi^2}\left[-4+\ln(M^2/\mu^2)+2\ln(M^2/\lambda^2)\right], \tag{64}$$

$$\delta_{\mathrm{cont}} = \frac{1}{12\pi^2}\left[4+3\ln(\mu^2/M^2)\right]. \tag{65}$$

Note that μ is the mass scale introduced by dimensional regularization and λ is the gluon mass regulating the infrared divergence. Thus, the sole effect of the order g^2 corrections is to renormalize the quark field and mass. If lattice NRQCD is to reproduce the low-energy physical predictions of full QCD, then the order g^2 corrections to the heavy-quark propagator in lattice NRQCD must also do no more than renormalize the heavy-quark field and mass to the appropriate order in v.

Explicit calculation shows that the heavy-quark self-energy in lattice NRQCD has a small v representation of the form

$$a\Sigma(p) \approx g^2\Big\{\Omega_0 + ip_4a\Omega_1 + \frac{\mathbf{p}^2a^2}{2Ma}\Omega_2 + \cdots\Big\}, \tag{66}$$

retaining only radiative corrections to the lowest-order terms in v as specified by the power counting rules of Ref. [2]. The on-mass-shell quark now satisfies a dispersion relation given by

$$\omega_0(\mathbf{p}) \approx i\left(-\frac{g^2}{a}\Omega_0 + \frac{\mathbf{p}^2}{2M}\left(1+g^2\Omega_1-g^2\Omega_2\right) + \cdots\right). \tag{67}$$

Defining $M_r = Z_mM$, where $Z_m = 1 - g^2\Omega_1 + g^2\Omega_2$ is the mass renormalization factor, and $\bar{p}_4 = p_4 + ig^2\Omega_0/a$, the inverse propagator for small v may be written

$$aG^{-1}(p) \approx Z_\psi \left(i\bar{p}_4 a + \frac{\mathbf{p}^2 a^2}{2M_r a} + \cdots \right), \qquad (68)$$

where $Z_\psi = 1 - g^2(\Omega_0 + \Omega_1)$ is the wave function renormalization parameter. Thus, the addition of a counterterm which shifts the energy by an overall amount $\bar{g}_r^2\Omega_0/a$ is needed in order to match the low-energy physical predictions of lattice NRQCD with those of QCD. Alternatively, one could simply shift the energies obtained in simulations using the action in Eq. 11 by an amount $\bar{g}_r^2\Omega_0/a$ for each heavy quark.

A more convenient set of renormalization parameters may be obtained by defining $Z_\psi = 1 - g^2 C$, $Z_m = 1 + g^2 B$, and $\bar{p}_4 = p_4 - ig^2 A/a$. The parameters A, B, and C can then be calculated using $A = -\Omega_0$, $B = \Omega_2 - \Omega_1$, and $C = \Omega_0 + \Omega_1$, where $\Omega_0 = a\Sigma(0)/g^2$, $\Omega_1 = -ia\partial_{p_4 a}\Sigma(0)/g^2$, and $\Omega_2 = 2Ma^2\partial_{\mathbf{p}^2 a^2}\Sigma(0)/g^2$. Because of the complexity of the NRQCD vertex factors, the derivatives in these expressions must be taken numerically. Four- and five-point formulas are applied in the differentiation; only points which satisfy $p_x = p_y = p_z$ are used since the self-energy can be computed much more quickly at such points.

Results for the energy shift parameter A and the mass renormalization parameter B are presented in Tables I and II, respectively. Both A and B are gauge invariant and infrared finite. The wave function renormalization parameter C has an infrared divergence of the form $-(\ln a^2\lambda^2)/6\pi^2$ as the gluon mass is taken to zero. This divergence is cancelled in physical quantities by an infrared divergence occurring in the quark-gluon vertex correction. Values for the infrared-finite portion of C are given in Table III. In these tables, the contributions from the quark-gluon loop and tadpole diagrams are given separately. Results using the simple and the improved gluonic actions are presented. Values for the stability parameter n are chosen such that the singularity in the quark propagator $Q(p)$ falls on the same side of the real axis in the complex p_4 plane for all allowed values of $\mathbf{p}$ and tends to move farther away from this real axis as $|\mathbf{p}|$ increases to its allowed maximum. For $aM \geq 2$, n is set to unity; for $1 \leq aM < 2$, $n = 2$ is used. These values of n ensure the stability of the evolution equation for the quark Green's function.

Contributions from the quark-gluon loop graph to the energy shift parameter A are small and decrease in magnitude as aM decreases. At large aM, there is little difference between the shifts obtained using the simple and improved gluonic actions. The tadpole contributions are large and contain power-law divergences which grow in magnitude as aM is decreased. Since high-momentum modes are more strongly damped in the improved gluon propagator, the ultraviolet-divergent tadpole terms are appreciably smaller in the case of the improved gluon action. These total downward shifts in the energy are

TABLE I. The energy shift parameter A for various values of the product of the bare heavy-quark mass M and the lattice spacing a. The contribution to A from the quark-gluon loop diagram of Fig. 2(a) is denoted by $A_i(A)$ for the improved gluon action of Eq. (23) and by $A_s(A)$ for the simple gluon action of Eq. (21). The contribution from the tadpole diagram of Fig. 2(b) is denoted by $A_i(B)$ and $A_s(B)$ for the improved and simple gluon actions, respectively. For $aM \geq 2$, the stability parameter n is set to unity; for $1 \leq aM < 2$, $n = 2$ is used. Extrapolation uncertainties are no larger than ± 0.0001.

aM	$A_i(A)$	$A_i(B)$	$A_s(A)$	$A_s(B)$
5.00	0.0417	0.1361	0.0414	0.1688
4.75	0.0407	0.1387	0.0403	0.1719
4.50	0.0397	0.1415	0.0391	0.1754
4.25	0.0385	0.1446	0.0377	0.1793
4.00	0.0372	0.1480	0.0363	0.1835
3.75	0.0358	0.1519	0.0347	0.1883
3.50	0.0342	0.1562	0.0329	0.1937
3.25	0.0325	0.1611	0.0309	0.1998
3.00	0.0306	0.1667	0.0288	0.2067
2.75	0.0284	0.1732	0.0263	0.2147
2.50	0.0261	0.1807	0.0237	0.2241
2.25	0.0234	0.1896	0.0208	0.2351
2.00	0.0206	0.2002	0.0176	0.2482
1.90	0.0199	0.2046	0.0168	0.2536
1.80	0.0185	0.2101	0.0154	0.2603
1.70	0.0172	0.2160	0.0139	0.2677
1.60	0.0158	0.2226	0.0124	0.2759
1.50	0.0143	0.2300	0.0108	0.2850
1.40	0.0129	0.2383	0.0092	0.2952
1.30	0.0114	0.2476	0.0076	0.3068
1.20	0.0100	0.2584	0.0061	0.3201
1.10	0.0086	0.2708	0.0047	0.3354
1.00	0.0075	0.2850	0.0036	0.3530

nearly the same as those obtained in Ref. [3] which used a much simpler heavy-quark action. Calculations of A using $c_j = 0$ for $j = 3, 4, 5, 6, 7$ reveal that contributions to this parameter from the spin-dependent interactions are small.

Contributions to the mass renormalization parameter B from the quark-gluon loop diagram are very small and do not vary proportionately with aM. For all values of aM, there is little difference between the results obtained using the simple and the improved gluon actions. The tadpole contributions are again large, growing in magnitude as aM is decreased. The tadpole terms in the case of the improved action are slightly smaller and contributions to this parameter from the spin-dependent interactions are small. The total values for B obtained here are appreciably larger than the order g^2 corrections to the mass renormalization calculated in Ref. [3] (see Ref. [10]).

The tadpole diagrams do not contribute to the heavy-quark wave function renormalization parameter C. The values for the infrared-finite portion of C are very small and become increasingly negative as aM is decreased. There is little difference between the results obtained using the simple and the improved gluonic actions. The magnitudes of the wave function renormalization corrections are much smaller than those obtained in Ref. [3] (see Ref. [10]).

The contributions to the energy shift and mass renormalization parameters from the link variable renormalization counterterm are given by

$$\delta A = u_0^{(2)} \left(1 + \frac{7}{2Ma}\right), \tag{69}$$

$$\delta B = u_0^{(2)} \left(\frac{2}{3} - \frac{1}{4nMa} + \frac{3}{M^2a^2}\right). \tag{70}$$

No change in the wave function renormalization occurs. As previously stated, the purpose of link variable renormalization is to enhance the similarities between lattice and continuum gauge-field operators, especially those depending on the cloverleaf electric and magnetic fields. Consequently, the counterterms introduced by this renormalization offset the large tadpole contributions which commonly afflict lattice perturbation theory, offering a means of improving its convergence. As shown in Table IV, the order g^2 corrections to the heavy-quark renormalization parameters are small once the mean-field corrections are taken into account. In this table, the value $u_0^{(2)} = -0.083$ obtained by evaluating Eq. (27) in perturbation theory for the simple gluonic action is used. For $\bar{g}_r^2 \sim 2$ and $a \sim 1$ GeV^{-1}, the b quark receives approximately a 1% lowest-order correction to its mass and the c quark receives about a 7% mass correction.

TABLE II. The heavy-quark mass renormalization parameter B for various values of the product of the bare heavy-quark mass M and the lattice spacing a. The contribution to B from the quark-gluon loop diagram of Fig. 2(a) is denoted by $B_i(A)$ for the improved gluon action of Eq. (23) and by $B_s(A)$ for the simple gluon action of Eq. (21). The contribution from the tadpole diagram of Fig. 2(b) is denoted by $B_i(B)$ and $B_s(B)$ for the improved and simple gluon actions, respectively. For $aM \geq 2$, the stability parameter n is set to unity; for $1 \leq aM < 2$, $n = 2$ is used. Extrapolation uncertainties are no larger than ± 0.0001 for the tadpole values and ± 0.0002 for the contributions from the quark-gluon loop diagram.

aM	$B_i(A)$	$B_i(B)$	$B_s(A)$	$B_s(B)$
5.00	−0.0024	0.0556	−0.0030	0.0697
4.75	−0.0016	0.0568	−0.0021	0.0712
4.50	−0.0008	0.0582	−0.0011	0.0728
4.25	0.0000	0.0599	−0.0002	0.0748
4.00	0.0009	0.0619	0.0008	0.0771
3.75	0.0018	0.0642	0.0019	0.0798
3.50	0.0028	0.0670	0.0030	0.0832
3.25	0.0039	0.0704	0.0042	0.0872
3.00	0.0049	0.0747	0.0054	0.0923
2.75	0.0059	0.0801	0.0065	0.0987
2.50	0.0069	0.0871	0.0076	0.1070
2.25	0.0077	0.0963	0.0085	0.1181
2.00	0.0080	0.1091	0.0089	0.1334
1.90	0.0076	0.1175	0.0083	0.1438
1.80	0.0077	0.1248	0.0084	0.1525
1.70	0.0077	0.1332	0.0084	0.1626
1.60	0.0076	0.1431	0.0083	0.1746
1.50	0.0073	0.1550	0.0079	0.1889
1.40	0.0068	0.1692	0.0073	0.2061
1.30	0.0060	0.1868	0.0064	0.2274
1.20	0.0048	0.2089	0.0051	0.2541
1.10	0.0032	0.2373	0.0032	0.2885
1.00	0.0010	0.2752	0.0007	0.3345

TABLE III. The infrared-finite portion of the heavy-quark wave function renormalization parameter C for various values of the product of the bare heavy-quark mass M and the lattice spacing a. The infrared-finite contribution to C from the quark-gluon loop diagram of Fig. 2(a) is denoted by C_i for the improved gluon action of Eq. (23) and by C_s for the simple gluon action of Eq. (21). The tadpole diagram of Fig. 2(b) does not contribute to this parameter. For $aM \geq 2$, the stability parameter n is set to unity; for $1 \leq aM < 2$, $n = 2$ is used. Extrapolation uncertainties are no larger than ± 0.0001.

aM	C_i	C_s
5.00	0.0032	0.0029
4.75	0.0018	0.0014
4.50	0.0002	−0.0004
4.25	−0.0015	−0.0023
4.00	−0.0033	−0.0044
3.75	−0.0054	−0.0067
3.50	−0.0077	−0.0092
3.25	−0.0102	−0.0120
3.00	−0.0131	−0.0152
2.75	−0.0163	−0.0187
2.50	−0.0199	−0.0226
2.25	−0.0239	−0.0270
2.00	−0.0285	−0.0319
1.90	−0.0300	−0.0335
1.80	−0.0322	−0.0358
1.70	−0.0345	−0.0382
1.60	−0.0369	−0.0408
1.50	−0.0395	−0.0435
1.40	−0.0422	−0.0464
1.30	−0.0450	−0.0493
1.20	−0.0480	−0.0524
1.10	−0.0511	−0.0555
1.00	−0.0542	−0.0587

TABLE IV. Tadpole improvement of the energy shift parameter A and mass renormalization parameter B for various values of the product of the bare mass M and the lattice spacing a. Results are given for the simple gluon action only. The renormalization parameters without tadpole improvement are denoted by A_s and B_s; the improved parameters are denoted by $\tilde{A}_s$ and $\tilde{B}_s$. The perturbative value $u_0^{(2)} = -0.083$ is used for the mean-field parameter.

aM	A_s	$\tilde{A}_s$	B_s	$\tilde{B}_s$
5.00	0.210	0.069	0.067	0.006
4.00	0.220	0.064	0.078	0.012
3.00	0.236	0.056	0.098	0.022
2.00	0.266	0.038	0.142	0.035
1.70	0.282	0.028	0.171	0.036
1.30	0.314	0.008	0.234	0.039
1.00	0.357	−0.017	0.335	0.041

V. CONCLUSION

Lattice NRQCD is an effective-field theory which promises to make possible high-precision numerical studies of heavy-quark systems. It is essentially a low-energy expansion of QCD in terms of the mean velocity of the heavy quarks in a typical heavy-quark hadron. To fully define lattice NRQCD, the coupling strengths of its interactions must be specified. These are determined by requiring that lattice NRQCD reproduces the low-energy physical results of continuum QCD. Since the role of these couplings is to absorb the relativistic effects arising from highly ultraviolet QCD processes, one expects that they may be computed to a good approximation using perturbation theory, provided the quark mass M is large enough.

The heavy-quark self-energy in nonrelativistic lattice QCD was calculated to $O(\alpha_s)$ in perturbation theory. An action which includes all spin-independent relativistic corrections to order v^2 and all spin-dependent corrections to order v^4 was used. The standard Wilson action and an improved multi-plaquette action were used for the gluons. Results for the mass and wave function renormalization and an overall energy shift were obtained. Contributions from the quark-gluon loop graph were found to be very small; however, the tadpole contributions were large. The values of these parameters will be needed in future numerical simulations of quarkonium. The effective couplings will also be needed; calculation of these quantities is in progress.

A tadpole improvement scheme in which all link variables are rescaled by a mean-field factor u_0 was also applied in perturbation theory. The main purpose of this link variable renormalization was to enhance the similarities between lattice and continuum gauge-field operators, especially those depending on the cloverleaf electric and magnetic fields. An important consequence of this scheme was a significant offsetting of the large tadpole contributions to the heavy-quark renormalization parameters. Using a perturbative approximation to the mean plaquette for u_0, the tadpole-improved heavy-quark renormalization parameters were shown to be small. This scheme offers a means of improving the convergence properties of lattice perturbation theory.

ACKNOWLEDGMENTS

I would like to thank G. Peter Lepage for many useful conversations. This work was supported by the Natural Sciences and Engineering Research Council of Canada and by the Department of Energy, Contract No. DE-AC03-76SF00515.

APPENDIX: FOURIER TRANSFORMS

The momentum-space representations of various components of the lattice NRQCD action are presented in this Appendix. Below, ζ functions are introduced and are defined by

$$\xi_A^{(r)}(k',k;q_1,\nu_1,b_1;\ldots;q_r,\nu_r,b_r) = g^r \zeta_A^{(r)}(k',k;q_1,\nu_1;\ldots;q_r,\nu_r)\, T^{b_1}\cdots T^{b_r}. \tag{A1}$$

Also note that $\bar{\delta}_{\mu\nu}$ is an "anti-Kronecker delta function" and is trivial when $\mu=\nu$ and unity otherwise.

In momentum space, the link variable becomes

$$\begin{aligned}U_\mu(k';k)&=a^4\sum_x e^{-i(k'-k)\cdot x}e^{ik_\mu a}\exp\left[iagA_\mu\left(x+\frac{a}{2}\hat{e}_\mu\right)\right]\\&=(2\pi)^4\delta^{(4)}(k'-k)e^{ia(k'_\mu+k_\mu)/2}+iag\int d(k',k;q)e^{ia(k'_\mu+k_\mu)/2}\tilde{A}_\mu(q)\\&\quad-\frac{a^2g^2}{2}\int d(k',k;q_1,q_2)e^{ia(k'_\mu+k_\mu)/2}\tilde{A}_\mu(q_1)\tilde{A}_\mu(q_2)\\&\quad-\frac{ia^3g^3}{6}\int d(k',k;q_1,q_2,q_3)e^{ia(k'_\mu+k_\mu)/2}\tilde{A}_\mu(q_1)\tilde{A}_\mu(q_2)\tilde{A}_\mu(q_3)+\cdots.\end{aligned}\tag{A2}$$

The momentum-space representation of $\Delta_\mu^{(\pm)}$ may be written

$$\begin{aligned}\zeta^{(0)}_{a\Delta_\mu^{(\pm)}}(k',k)&=i\sin\left[\frac{a}{2}(k'+k)_\mu\right],\\\zeta^{(1)}_{a\Delta_\mu^{(\pm)}}(k',k;q_1,\nu_1)&=ia\cos\left[\frac{a}{2}(k'+k)_\mu\right]\delta_{\mu,\nu_1},\\\zeta^{(2)}_{a\Delta_\mu^{(\pm)}}(k',k;q_1,\nu_1;q_2,\nu_2)&=-i\frac{a^2}{2}\sin\left[\frac{a}{2}(k'+k)_\mu\right]\delta_{\mu,\nu_1}\delta_{\mu,\nu_2},\\\zeta^{(3)}_{a\Delta_\mu^{(\pm)}}(k',k;q_1,\nu_1;q_2,\nu_2;q_3,\nu_3)&=-i\frac{a^3}{6}\cos\left[\frac{a}{2}(k'+k)_\mu\right]\delta_{\mu,\nu_1}\delta_{\mu,\nu_2}\delta_{\mu,\nu_3}.\end{aligned}\tag{A3}$$

The improved symmetric derivative has the momentum-space representation

$$\begin{aligned}\zeta^{(0)}_{a\tilde{\Delta}_\mu^{(\pm)}}(k',k)&=i\left(\frac{4}{3}\sin\left[\frac{a}{2}(k'+k)_\mu\right]-\frac{1}{6}\sin\left[a(k'+k)_\mu\right]\right),\\\zeta^{(1)}_{a\tilde{\Delta}_\mu^{(\pm)}}(k',k;q_1,\nu_1)&=i\frac{a}{3}\delta_{\mu,\nu_1}\left(4\cos\left[\frac{a}{2}(k'+k)_\mu\right]-\cos\left[a(k'+k)_\mu\right]\cos\left(\frac{a}{2}q_{1\mu}\right)\right),\\\zeta^{(2)}_{a\tilde{\Delta}_\mu^{(\pm)}}(k',k;q_1,\nu_1;q_2,\nu_2)&=ia^2\delta_{\mu,\nu_1}\delta_{\mu,\nu_2}\left(-\frac{2}{3}\sin\left[\frac{a}{2}(k'+k)_\mu\right]+\frac{1}{3}\sin\left[a(k'+k)_\mu\right]\cos\left(\frac{a}{2}q_{1\mu}\right)\cos\left(\frac{a}{2}q_{2\mu}\right)\right.\\&\quad\left.+\frac{1}{6}\cos\left[a(k'+k)_\mu\right]\sin\left[\frac{a}{2}(q_1-q_2)_\mu\right]\right),\\\zeta^{(3)}_{a\tilde{\Delta}_\mu^{(\pm)}}(k',k;q_1,\nu_1;q_2,\nu_2;q_3,\nu_3)&=ia^3\delta_{\mu,\nu_1}\delta_{\mu,\nu_2}\delta_{\mu,\nu_3}\left(-\frac{2}{9}\cos\left[\frac{a}{2}(k'+k)_\mu\right]+\frac{1}{18}\cos\left[a(k'+k)_\mu\right]\cos\left[\frac{a}{2}(k'-k)_\mu\right]\right.\\&\quad\left.+\frac{1}{6}\cos\left[a\left(k'+k+\frac{1}{2}q_1-\frac{1}{2}q_3\right)_\mu\right]\cos\left(\frac{a}{2}q_{2\mu}\right)\right).\end{aligned}\tag{A4}$$

The Fourier transform of the lattice Laplacian may be written

$$\begin{aligned}
\zeta^{(0)}_{a^2\Delta^{(2)}}(k',k) &= -4\sum_{j=1}^{3}\sin^2\Big[\frac{a}{4}(k'+k)_j\Big],\\
\zeta^{(1)}_{a^2\Delta^{(2)}}(k',k;q_1,\nu_1) &= -2a\sin\Big[\frac{a}{2}(k'+k)_{\nu_1}\Big]\bar{\delta}_{4,\nu_1},\\
\zeta^{(2)}_{a^2\Delta^{(2)}}(k',k;q_1,\nu_1;q_2,\nu_2) &= -a^2\cos\Big[\frac{a}{2}(k'+k)_{\nu_1}\Big]\delta_{\nu_1,\nu_2}\bar{\delta}_{4,\nu_1},\\
\zeta^{(3)}_{a^2\Delta^{(2)}}(k',k;q_1,\nu_1;q_2,\nu_2;q_3,\nu_3) &= \frac{a^3}{3}\sin\Big[\frac{a}{2}(k'+k)_{\nu_1}\Big]\delta_{\nu_1,\nu_2}\delta_{\nu_2,\nu_3}\bar{\delta}_{4,\nu_1}.
\end{aligned} \tag{A5}$$

Similarly, for the improved Laplacian,

$$\begin{aligned}
\zeta^{(0)}_{a^2\tilde{\Delta}^{(2)}}(k',k) &= -4\sum_{j=1}^{3}\left(\sin^2\left[\frac{a}{4}(k'+k)_j\right]+\frac{1}{3}\sin^4\left[\frac{a}{4}(k'+k)_j\right]\right),\\
\zeta^{(1)}_{a^2\tilde{\Delta}^{(2)}}(k',k;q_1,\nu_1) &= \frac{a}{3}\bar{\delta}_{4,\nu_1}\left(-8\sin\left[\frac{a}{2}(k'+k)_{\nu_1}\right]+\sin\big[a(k'+k)_{\nu_1}\big]\cos\left(\frac{a}{2}q_{1\nu_1}\right)\right),
\end{aligned}$$

$$\begin{aligned}
\zeta^{(2)}_{a^2\tilde{\Delta}^{(2)}}(k',k;q_1,\nu_1;q_2,\nu_2) &= a^2\delta_{\nu_1,\nu_2}\bar{\delta}_{4,\nu_1}\left(-\frac{4}{3}\cos\left[\frac{a}{2}(k'+k)_{\nu_1}\right]+\frac{1}{3}\cos\big[a(k'+k)_{\nu_1}\big]\cos\left(\frac{a}{2}q_{1\nu_1}\right)\cos\left(\frac{a}{2}q_{2\nu_1}\right)\right.\\
&\qquad\left.-\frac{1}{6}\sin\Big[a(k'+k)_{\nu_1}\Big]\sin\big[\frac{a}{2}(q_1-q_2)_{\nu_1}\big]\right),
\end{aligned} \tag{A6}$$

$$\begin{aligned}
\zeta^{(3)}_{a^2\tilde{\Delta}^{(2)}}(k',k;q_1,\nu_1;q_2,\nu_2;q_3,\nu_3) &= a^3\delta_{\nu_1,\nu_2}\delta_{\nu_2,\nu_3}\bar{\delta}_{4,\nu_1}\left(\frac{4}{9}\sin\left[\frac{a}{2}(k'+k)_{\nu_1}\right]-\frac{1}{6}\sin\left[a\left(k'+k+\frac{1}{2}q_1-\frac{1}{2}q_3\right)_{\nu_1}\right]\cos\left(\frac{a}{2}q_{2\nu_2}\right)\right.\\
&\qquad\left.-\frac{1}{18}\sin\big[a(k'+k)_{\nu_1}\big]\cos\left[\frac{a}{2}(k'-k)_{\nu_1}\right]\right).
\end{aligned}$$

Another important operator is the cloverleaf field strength tensor. Its Fourier transform is given by

$$\begin{aligned}
F_{\mu\nu}(k';k) &= a^4\sum_x e^{-i(k'-k)\cdot x}F_{\mu\nu}(x)\\
&= -\frac{i}{a}\sum_b\int d(k',k;q)\ \big[f^A_{\mu\nu}(q)\ \tilde{A}^b_\nu(q)-f^A_{\nu\mu}(q)\ \tilde{A}^b_\mu(q)\big]\ T^b\\
&\quad+ig\sum_{b_1b_2}\int d(k',k;q_1,q_2)\ T^{b_1}T^{b_2}\Big\{f^B_{\mu\nu}(q_1,q_2)\ \tilde{A}^{b_1}_\nu(q_1)\tilde{A}^{b_2}_\nu(q_2)\\
&\qquad-f^B_{\nu\mu}(q_1,q_2)\tilde{A}^{b_1}_\mu(q_1)\tilde{A}^{b_2}_\mu(q_2)+f^C_{\mu\nu}(q_1,q_2)\tilde{A}^{b_1}_\mu(q_1)\tilde{A}^{b_2}_\nu(q_2)\\
&\qquad-f^C_{\nu\mu}(q_1,q_2)\tilde{A}^{b_1}_\nu(q_1)\tilde{A}^{b_2}_\mu(q_2)\Big\}\\
&\quad-iag^2\sum_{b_1b_2b_3}\int d(k',k;q_1,q_2,q_3)\ \Big(T^{b_1}T^{b_2}T^{b_3}-\frac{1}{3}\mathrm{Tr}T^{b_1}T^{b_2}T^{b_3}\Big)\\
&\qquad\times\Big\{-f^F_{\mu\nu}(q_1,q_2,q_3)\ \tilde{A}^{b_1}_\nu(q_1)\tilde{A}^{b_2}_\mu(q_2)\tilde{A}^{b_3}_\nu(q_3)+f^D_{\mu\nu}(q_1,q_2,q_3)\ \tilde{A}^{b_1}_\mu(q_1)\tilde{A}^{b_2}_\mu(q_2)\tilde{A}^{b_3}_\mu(q_3)\\
&\qquad-f^D_{\nu\mu}(q_1,q_2,q_3)\ \tilde{A}^{b_1}_\nu(q_1)\tilde{A}^{b_2}_\nu(q_2)\tilde{A}^{b_3}_\nu(q_3)-f^E_{\nu\mu}(q_1,q_2,q_3)\ \tilde{A}^{b_1}_\mu(q_1)\tilde{A}^{b_2}_\mu(q_2)\tilde{A}^{b_3}_\nu(q_3)\\
&\qquad-f^E_{\nu\mu}(q_3,q_2,q_1)\ \tilde{A}^{b_1}_\nu(q_1)\tilde{A}^{b_2}_\mu(q_2)\tilde{A}^{b_3}_\mu(q_3)+f^E_{\mu\nu}(q_1,q_2,q_3)\ \tilde{A}^{b_1}_\nu(q_1)\tilde{A}^{b_2}_\nu(q_2)\tilde{A}^{b_3}_\mu(q_3)\\
&\qquad+f^E_{\mu\nu}(q_3,q_2,q_1)\ \tilde{A}^{b_1}_\mu(q_1)\tilde{A}^{b_2}_\nu(q_2)\tilde{A}^{b_3}_\nu(q_3)+f^F_{\nu\mu}(q_1,q_2,q_3)\ \tilde{A}^{b_1}_\mu(q_1)\tilde{A}^{b_2}_\nu(q_2)\tilde{A}^{b_3}_\mu(q_3)\Big\}\\
&\quad+O(g^3)
\end{aligned} \tag{A7}$$

where

$$f^A_{\mu\nu}(q) = \sin(aq_\mu)\cos\left(\frac{a}{2}q_\nu\right),$$

$$f^B_{\mu\nu}(q_1,q_2) = \cos\left[\frac{a}{2}(q_1+q_2)_\mu\right]\sin\left[\frac{a}{2}(q_1+q_2)_\nu\right]\sin\left[\frac{a}{2}(q_1-q_2)_\mu\right],$$

$$f^C_{\mu\nu}(q_1,q_2) = \frac{1}{2}\left[\cos\left(\frac{a}{2}q_{1\mu}\right)\cos\left(aq_{1\nu}+\frac{a}{2}q_{2\nu}\right)+\cos\left(\frac{a}{2}q_{2\nu}\right)\cos\left(aq_{2\mu}+\frac{a}{2}q_{1\mu}\right)\right.$$
$$\left.+\cos\left(aq_{2\mu}+\frac{a}{2}q_{1\mu}\right)\cos\left(aq_{1\nu}+\frac{a}{2}q_{2\nu}\right)-\cos\left(\frac{a}{2}q_{1\mu}\right)\cos\left(\frac{a}{2}q_{2\nu}\right)\right],$$

$$f^D_{\mu\nu}(q_1,q_2,q_3) = \cos\left[\frac{a}{2}(q_1+q_2+q_3)_\mu\right]\left\{\frac{1}{6}\sin\left[a(q_1+q_2+q_3)_\nu\right]\right. \tag{A8}$$
$$\left.-\cos\left[\frac{a}{2}(q_1+q_2+q_3)_\nu\right]\cos\left[\frac{a}{2}(q_1-q_3)_\nu\right]\sin\left(\frac{a}{2}q_{2\nu}\right)\right\},$$

$$f^E_{\mu\nu}(q_1,q_2,q_3) = \cos\left[\frac{a}{2}(q_1+q_2+q_3)_\mu\right]\cos\left[\frac{a}{2}(q_1+q_2+q_3)_\nu\right]\cos\left[\frac{a}{2}(q_1+q_2)_\mu\right]\sin\left(\frac{a}{2}q_{3\nu}\right)$$
$$+\frac{1}{2}\cos\left[a\left(q_2+\frac{1}{2}q_3\right)_\mu\right]\sin\left[\frac{a}{2}(q_1+q_2)_\nu\right],$$

$$f^F_{\mu\nu}(q_1,q_2,q_3) = \cos\left[\frac{a}{2}(q_1+q_2+q_3)_\mu\right]\sin\left[a\left(\frac{1}{2}q_1+q_2+\frac{1}{2}q_3\right)_\nu\right]\cos\left[\frac{a}{2}(q_1-q_3)_\mu\right].$$

Using $\tilde{A}^b_\mu(q)^* = \tilde{A}^b_\mu(-q)$, one can easily check that $F^b_{\mu\nu}(k';k)^* = F^b_{\mu\nu}(-k';-k)$. Furthermore, $F_{\mu\nu}(k';k) = -F_{\nu\mu}(k';k)$, as required. Note the absence of a $\mathrm{Tr}T^{b_1}T^{b_2}$ term in the order g coefficient.

The Fourier transform of the improved cloverleaf field strength tensor has the same form as that for $F_{\mu\nu}$, but the functions $f^A_{\mu\nu},\ldots$ must be replaced by the functions

$$\tilde{f}^A_{\mu\nu}(q) = \frac{1}{3}\left(5-\cos(aq_\mu)-\cos(aq_\nu)\right)f^A_{\mu\nu}(q),$$

$$\tilde{f}^B_{\mu\nu}(q_1,q_2) = \frac{1}{3}\left\{\left(5-\cos\left[a(q_1+q_2)_\mu\right]-\cos\left[a(q_1+q_2)_\nu\right]\right)f^B_{\mu\nu}(q_1,q_2)\right.$$
$$\left.-\sin\left[a\left(q_1+\frac{1}{2}q_2\right)_\nu\right]f^A_{\mu\nu}(q_1)+\sin\left[a\left(\frac{1}{2}q_1+q_2\right)_\nu\right]f^A_{\mu\nu}(q_2)\right\},$$

$$\tilde{f}^C_{\mu\nu}(q_1,q_2) = \frac{1}{3}\left\{\left(5-\cos\left[a(q_1+q_2)_\mu\right]-\cos\left[a(q_1+q_2)_\nu\right]\right)f^C_{\mu\nu}(q_1,q_2)\right.$$
$$\left.+\sin\left[a\left(q_1+\frac{1}{2}q_2\right)_\nu\right]f^A_{\nu\mu}(q_1)+\sin\left[a\left(\frac{1}{2}q_1+q_2\right)_\mu\right]f^A_{\mu\nu}(q_2)\right\},$$

$$\tilde{f}^D_{\mu\nu}(q_1,q_2,q_3) = \frac{1}{3}\Bigg\{ \big(5-\cos\big[a(q_1+q_2+q_3)_\mu\big]-\cos\big[a(q_1+q_2+q_3)_\nu\big]\big) f^D_{\mu\nu}(q_1,q_2,q_3)$$
$$+\sin\left[a\left(q_1+q_2+\frac{1}{2}q_3\right)_\mu\right] f^B_{\nu\mu}(q_1,q_2) - \sin\left[a\left(\frac{1}{2}q_1+q_2+q_3\right)_\mu\right] f^B_{\nu\mu}(q_2,q_3)$$
$$-\frac{1}{2}\cos\left[a\left(q_1+\frac{1}{2}q_2+\frac{1}{2}q_3\right)_\mu\right] f^A_{\nu\mu}(q_1) - \frac{1}{2}\cos\left[a\left(\frac{1}{2}q_1+\frac{1}{2}q_2+q_3\right)_\mu\right] f^A_{\nu\mu}(q_3) \qquad \text{(A9)}$$
$$+\cos\left[a\left(\frac{1}{2}q_1+q_2+\frac{1}{2}q_3\right)_\mu\right] f^A_{\nu\mu}(q_2)\Bigg\},$$

$$\tilde{f}^E_{\mu\nu}(q_1,q_2,q_3) = \frac{1}{3}\Bigg\{ \big(5-\cos\big[a(q_1+q_2+q_3)_\mu\big]-\cos\big[a(q_1+q_2+q_3)_\nu\big]\big) f^E_{\mu\nu}(q_1,q_2,q_3)$$
$$-\sin\left[a\left(q_1+q_2+\frac{1}{2}q_3\right)_\mu\right] f^B_{\mu\nu}(q_1,q_2) - \sin\left[a\left(\frac{1}{2}q_1+q_2+q_3\right)_\nu\right] f^C_{\nu\mu}(q_2,q_3)$$
$$-\frac{1}{2}\cos\left[a\left(\frac{1}{2}q_1+\frac{1}{2}q_2+q_3\right)_\nu\right] f^A_{\nu\mu}(q_3)\Bigg\},$$

$$\tilde{f}^F_{\mu\nu}(q_1,q_2,q_3) = \frac{1}{3}\Bigg\{ \big(5-\cos\big[a(q_1+q_2+q_3)_\mu\big]-\cos\big[a(q_1+q_2+q_3)_\nu\big]\big) f^F_{\mu\nu}(q_1,q_2,q_3)$$
$$-\sin\left[a\left(q_1+q_2+\frac{1}{2}q_3\right)_\nu\right] f^C_{\nu\mu}(q_1,q_2) - \sin\left[a\left(\frac{1}{2}q_1+q_2+q_3\right)_\nu\right] f^C_{\mu\nu}(q_2,q_3)$$
$$-\cos\left[a\left(\frac{1}{2}q_1+q_2+\frac{1}{2}q_3\right)_\nu\right] f^A_{\nu\mu}(q_2)\Bigg\}.$$

[1] B.A. Thacker and G. Peter Lepage, Phys. Rev. D **43**, 196 (1991).

[2] G. Peter Lepage, Lorenzo Magnea, Charles Nakhleh, Ulrika Magnea, and Kent Hornbostel, Phys. Rev. D **46**, 4052 (1992).

[3] C. T. H. Davies and B. A. Thacker, Phys. Rev. D **45**, 915 (1992).

[4] J. Mandula, G. Zweig, and J. Govaerts, Nucl. Phys. **B228**, 109 (1983).

[5] David G. Boulware, Ann. Phys. (N.Y.) **56**, 140 (1970).

[6] L.D. Faddeev and V.N. Popov, Phys. Lett. **25B**, 29 (1967).

[7] Hikaru Kawai, Ryuichi Nakayama, and Koichi Seo, Nucl. Phys. **B189**, 40 (1981).

[8] G. Peter Lepage and Paul B. Mackenzie, Phys. Rev. D **48**, 2250 (1993).

[9] M. Lüscher and P. Weisz, Nucl. Phys. **B266**, 309 (1986).

[10] Note that in terms of the parameters A, B, A_S, and Z defined in Ref. [3], the order g^2 corrections to the mass and wave function renormalization are given by $aA + B$ and $Z - aA_S$, respectively. See also Table II in Ref. [2].